Journal of Constructional Steel Research 89 (2013) 21–29

Contents lists available at ScienceDirect

Journal of Constructional Steel Research

Influence of surface integrity on the fatigue strength of high-strength steels

Heikki Remes [a,*], Eero Korhonen [a], Pauli Lehto [a], Jani Romanoff [a], Ari Niemelä [b], Pasi Hiltunen [b], Tuomo Kontkanen [b]

[a] Department of Applied Mechanics, School of Engineering, Aalto University, Espoo, Finland
[b] STX Finland, Turku Shipyard, Turku, Finland

ARTICLE INFO

Article history:
Received 16 April 2013
Accepted 7 June 2013
Available online 7 July 2013

Keywords:
Fatigue strength
High-strength steel
Surface integrity
Large-scale testing
Ship structure

ABSTRACT

This paper investigates experimentally the influence of surface integrity on the fatigue strength of high-strength steel used in large structures. The investigation utilises large-scale specimens of the balcony openings of a cruise ship. The test specimens, which have a dog-bone shape and yield strength of 355 MPa, 460 MPa, or 690 MPa, are cut by plasma. After the cutting, the specimens are treated by grinding or by grinding followed by sandblasting, i.e. using post-cutting treatments that are suitable for shipyard conditions. The resulting surface roughness, hardness profile, and residual stress are measured. Fatigue tests with a load ratio of $R = 0.1$ are carried out until the final failure of the specimens. The investigation shows that post-cutting treatments suitable for shipyard conditions can considerably increase the fatigue strength of high-strength steel used in opening corners of a large-scale structure. Sandblasting after grinding increases the surface roughness, but reduces the fatigue strength only slightly.

1. Introduction

During recent years, increasing interest has been shown in new structural alternatives that improve energy efficiency and product competitiveness. For instance, the general arrangement of cruise and passenger ships has undergone dramatic changes and large openings are included in the load-carrying side structures, as illustrated in Fig. 1. The large balcony openings result in more comfortable cabins, but at the same the corners of these openings have become more strength-critical.

While the static strength can be increased by using high-strength steel, the fatigue strength of large structures such as ships does not increase at the same rate as the yield or ultimate strength of the material; see e.g. [1–3]. This is due to the fact that the cutting and welding of steel plates with conventional production technology introduces crack-like surface defects. Positioning the weld seams away from the high-stress areas can solve this problem partially, but the existence of the cut surface is still a problem to be solved. The production-induced surface defect acts as an initial crack for the fatigue crack growth. If the defects have a certain size, around 0.1 mm, the macro crack propagation dominates the fatigue process over the crack initiation [4], which leads to the loss of the benefits of high-strength steel, as illustrated in Fig. 2. If surface treatment is applied after the plate cutting, the size of the defects is significantly smaller and the high-strength steel can be better utilised in fatigue-loaded structures.

The influence of surface treatments and different processing methods on fatigue strength has been discussed, for example, by Murakami and Endo [5], Sasahara [6], Sperle [4], Gao et al. [7], and Ryu et al. [8]. These investigations show that in addition to the base material yield strength [9], the main parameters which affect the fatigue strength are the surface roughness, microscopic notch radius, hardness, and residual stresses. For favourable surface conditions, a significant fatigue strength improvement was observed in the case of small-scale specimens. However, the direct application of these results to large structures is very difficult or impossible, since the main parameters that have an effect are very sensitive to the processing method and the small-scale specimen is not able to capture the influence of the whole production process on the surface integrity and fatigue strength.

The aim of this study is to examine the influence of surface integrity on the fatigue strength of high-strength steel when production processes suitable for the construction of a large steel structure are considered. A case structure, i.e. a cruise ship side structure with a balcony opening, is applied in order to include all the manufacturing steps of a realistic production environment. Steels with a nominal yield strength of 460 MPa and 690 MPa are considered, and compared with the reference material with a yield strength of 355 MPa. The reference material represents the high-strength steel commonly used in shipbuilding. Large-scale specimens applied in the investigations are first plasma cut to a dog-bone shape simulating a balcony opening of a cruise ship. Then the specimens are grinded and finally sandblasted, which is

* Corresponding author at: Department of Applied Mechanics, School of Engineering, Aalto University, P.O. BOX 15300, FIN-00076 Aalto, Finland. Tel.: +358 407025268.
E-mail address: heikki.remes@aalto.fi (H. Remes).

0143-974X/$ – see front matter © 2013 Elsevier Ltd. All rights reserved.
http://dx.doi.org/10.1016/j.jcsr.2013.06.003

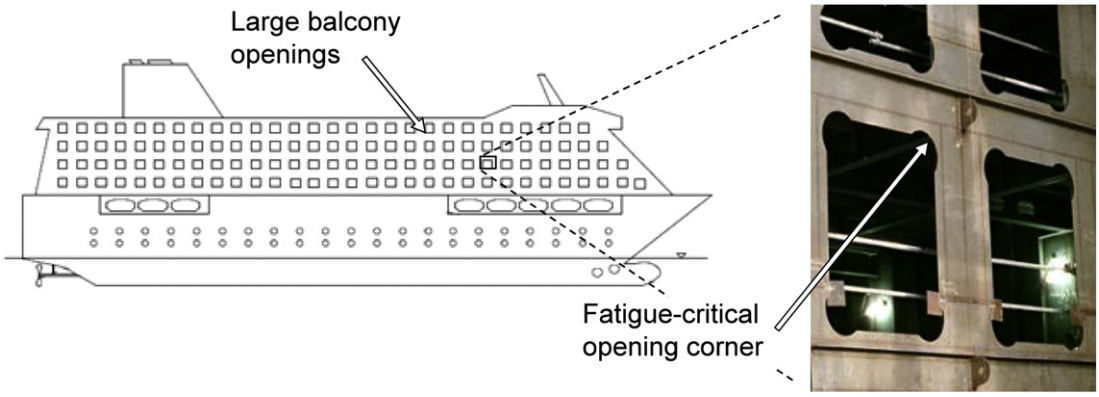

Fig. 1. An example of fatigue-critical structural detail in a large structure: the corner of the balcony opening in the side structure of a cruise ship.

required for painting. The specimens are fatigue tested and the test results are compared with the surface integrity, which is defined by the geometry, hardness, and residual stress measurements.

2. Large-scale specimen for the balcony opening of a cruise ship

The balcony openings typically fail under the maximum principal stress [10]. This stress is caused by the global hull girder under shear force and bending moment. Depending on the ratio of the shear force and bending moment, the direction of the principal stress σ_{11} and fatigue critical location in the window opening changes, as shown in Fig. 3. However, the failure always occurs in the direction of the principal stress. Therefore, in the testing the problem was simplified and the axially loaded dog-bone specimens were considered in the manner shown in Fig. 4. The radius of the specimens was 500 mm, i.e. the order of a typical radius for a balcony opening. In the case of the axially loaded test specimen, this radius means a stress concentration factor of $K_t = 1.02$. Thus, the influence of stress concentration was neglected and the analyses of the results were based on the nominal stress, $\sigma = F/A$, of the test cross-section. The width of the specimen at the narrowest cross-section was 30 mm, while the thickness was 15 mm or 17 mm.

In all the specimens, the corner between the cut edges and plate surfaces was grinded using shipyard production methods in order to omit the stress concentration of the sharp corner of the cut plate. In the first set of specimens, this was all that was done after the plasma cutting. In the second set, the plasma-cut edges and rolled surface were grinded. In the third set, after plasma cutting and grinding, the specimens were sandblasted to simulate the preparation of the steel plate for painting. These three sets of the specimens correspond to the different manufacturing phases: plate cutting, post-cutting treatment, and sandblasting before painting. Later, these sets are called untreated, grinded, and sandblasted specimens, respectively. The steel materials were produced by Ruukki, S460ML (EN10025-4:2004) and S690QL (EN10025-6:2009) with nominal yield strengths of 460 MPa and 690 MPa, respectively. As a reference, a specimen set with a 355 MPa yield strength was used (NVA-36; DNV 2005). This led to seven series of specimens and a total of 50 specimens, as shown in Table 1.

3. Experiments

3.1. Surface geometry measurements

The size of the surface defects was measured using surface roughness measurements according to SFS-EN ISO 4288 [11]. The measurements were carried out for the rolled plate surface and specimen edge along three different lines, i.e. at the edges and centre of the cut edge, as illustrated in Fig. 5. The tests were carried out using the replica technique and Surface Roughness Tester TR200 and Taylor Hobson Surtronic 3+ -devices. Both the arithmetical average, R_a, and the five largest peak-to-peak average, R_z, were defined. The notch radius was measured by fitting a circle to the measured surface height profile shown in Fig. 6.

3.2. Microstructural analysis and hardness measurements

Microstructural changes in the treated surfaces were analysed by producing macro samples and carrying out Vickers hardness measurements of those. The measurements were performed for each test series according to SFS-EN ISO-6507 [12]. The specimens were manufactured from the dog-bone specimens with a water-cooled abrasive cutter. As shown in Fig. 5, the hardness measurements

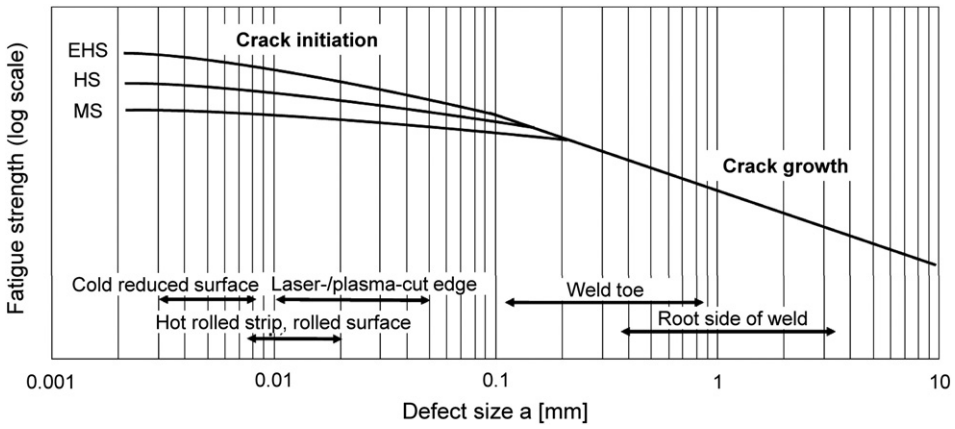

Fig. 2. Influence of the surface defect size on fatigue strength of extra-high-strength (EHS), high-strength (HS), and mild (MS) steels [4].

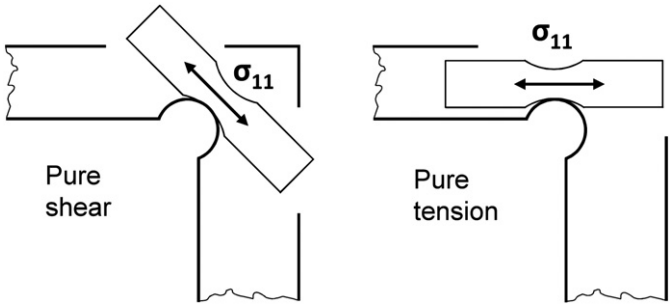

Fig. 3. Large-scale dog-bone specimen simulating the first principal stress at the opening corner under shear and tension loading.

were carried out for both the edge of the specimen cross-section, which was affected by the various treatments, and in the middle, which was unaffected by these. For the comparison of the results, the yield strength of the material was estimated from the Vickers hardness values by using the relation $\sigma_y = \mathrm{HV1} * k$, where k is a hardness conversion factor varying between 2 and 3 [13]. In the present study, a value of 2.5 was applied.

3.3. Residual stress measurements

Residual stresses were measured from the plate surface and the plasma-cut edge, as shown in Fig. 5. The specimen surfaces were cleaned with a HCL + C6H12N4 solution prior to the measurements. The X-ray diffraction technique with the modified χ-method ($\sin 2\psi$) was used for stress determination in accordance with the EN 15305 standard [14]. A Stresstech xStress 3000 G2R X-ray diffractometer with CrKα radiation (29.3 kV, 6.5 mA) was used for the residual stress measurements with a circular collimator with a diameter of 3 mm. The measurement was carried out at multiple inclinations; see Appendix A. Then the residual stress was determined by Bragg's law with the plane stress assumption as a result of the shallow penetration depth, i.e. 5.8 μm for ferritic steels according to EN 15305 [14]. The Young's modulus and Poisson's ratio used for the determination of the residual stress were $E = 211$ GPa and $\nu = 0.3$, respectively.

3.4. Fatigue tests

The fatigue tests were carried out using cyclic tensile tests with a load ratio $R = 0.1$. As shown in Fig. 7, the specimens were fixed to hinged clamping jaws that allowed rotation of the specimen to avoid secondary bending. The frequency of the test system was 1.8–3.5 Hz, depending on the load level defined for the test. The run-out point was defined at two million cycles. The specimens were instrumented with strain gauges on both sides of the specimens to verify that secondary bending was not present during the experiment. The test was force-controlled and stopped at complete failure of the specimen. After the fatigue tests, the fracture surfaces were analysed to identify the location of the fatigue crack initiation. Prior to the investigation, the fracture surfaces were cleaned using a HCL + $C_6H_{12}N_4$ solution.

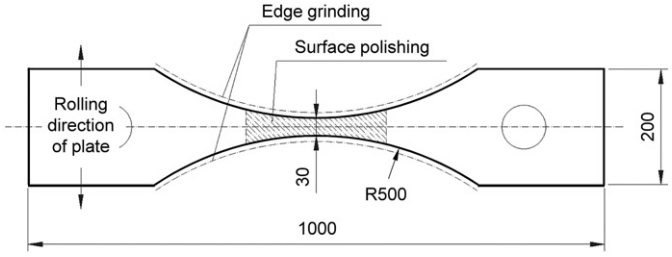

Fig. 4. The dimensions of the dog-bone specimen in millimetres.

Table 1
Number of specimens applied in the test programme.

Yield strength[a] [MPa]	Surface treatment after plasma cutting of the plate		
	Untreated	Grinded	Sandblasted
355	–	5	–
460	5	5	5
690	10	10	10

[a] Nominal yield strength of the material.

Macroscopic images of the fracture surfaces were taken using a digital single-lens reflex (dSLR) camera. From those images areas of interest were identified for closer examination. Higher-magnification images were taken using a microscope.

4. Results

4.1. Surface roughness

Examples of surface profiles and extracted surface roughness values for the various surface conditions are presented in Figs. 8 and 9, respectively. The surface profile of the grinded surface is considerably lower than those of the plasma-cut and sandblasted ones. This resulted in the lowest roughness values for the grinded surfaces, as shown in Fig. 9. Sandblasting causes the highest variations in surface profiles and thus, the surface roughness values are the highest, even beyond the rolled surfaces produced by the steel mill. On the other hand, the sandblasted surface was very homogenous and the averaged notch radius is larger than that of the grinded or plasma-cut surfaces.

4.2. Microstructure and hardness

The plasma cutting affected the material close to the plate edge, as shown in Fig. 10. On the basis of the hardness measurements, shown in Fig. 11, the heat-affected zone (HAZ) is about 0.5–1 mm wide, being slightly larger for the specimens with a lower yield strength. The hardness measurements also show that the transition zone between the HAZ and base material is wider for the specimens with a lower yield strength. In the case of the 690 MPa steel, the rapid change in the hardness profile indicates a very narrow transition zone. Grinding and sandblasting do not affect the hardness or width of the HAZ significantly. Regardless of the base material, the maximum hardness value is between 460HV1 and 510HV1. When these values are compared to the base material values below 300HV1, which are also shown in Table 2, it is evident that the surface of the cut edges has a considerably higher yield strength than that inside the specimen.

4.3. Residual stresses

The residual stresses for the rolled plate surface and plasma-cut plate edge are given in Fig. 12. Compressive residual stresses are present in the rolled surface of the untreated specimen. The heat effect of plasma cutting has slightly increased the residual stress on the plate edge. Irrespective of the material yield strength, grinding induced significant compressive residual stresses on both the rolled surface and the plate edge. For the rolled surface, sandblasting performed after grinding relaxed the residual stresses to a level close to the untreated state. Stress relaxation was also observed for the plasma-cut plate edge, but to a lesser degree. Complete measurement results are presented in Appendix A.

4.4. Fatigue strength

Fatigue test results for the grinded specimens are presented in Fig. 13; a 50% probability of survival is considered because of the limited number of tests. When the grinded specimens are considered, a considerable increase in the fatigue strength is found for the

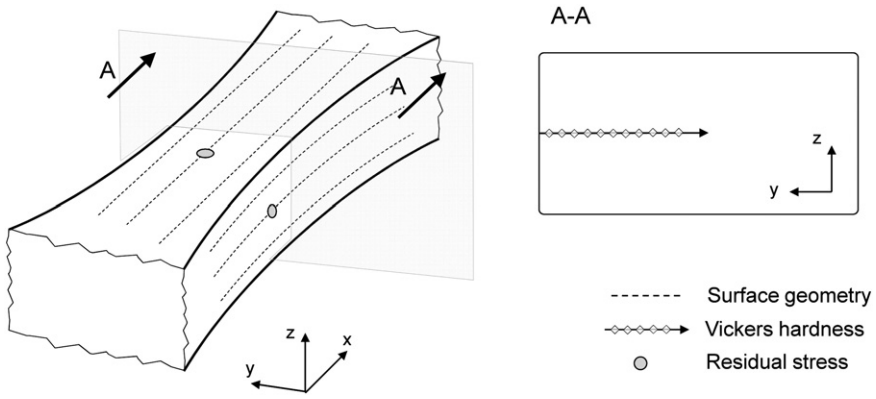

Fig. 5. The locations of the surface geometry, hardness, and residual stress measurements.

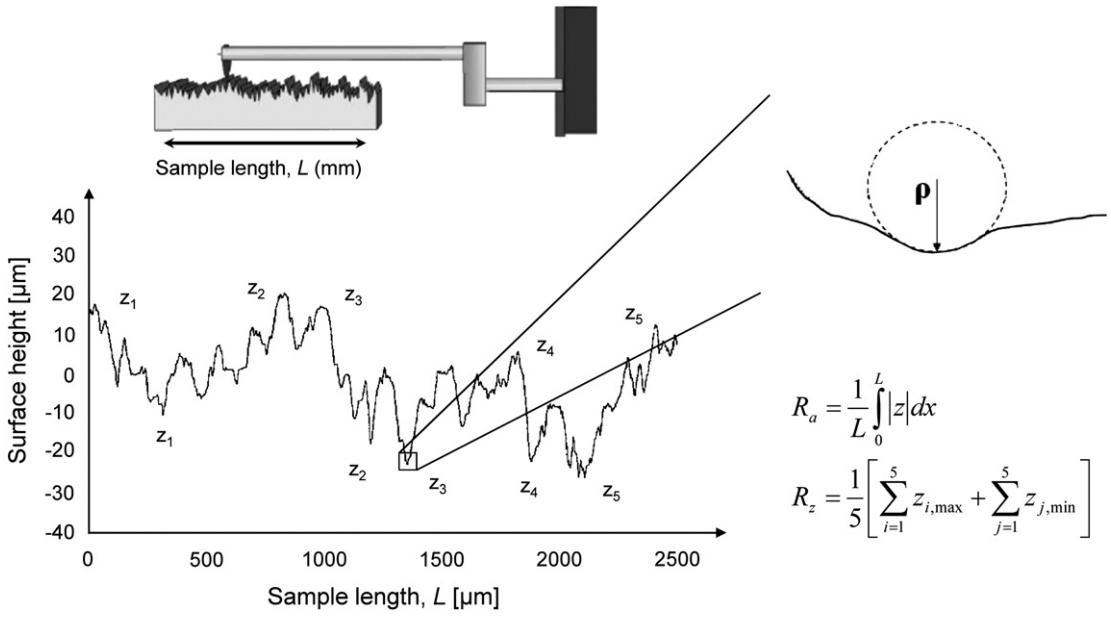

Fig. 6. Surface geometry measurements defining surface roughness, R_a and R_z, and the microscopic notch radius ρ.

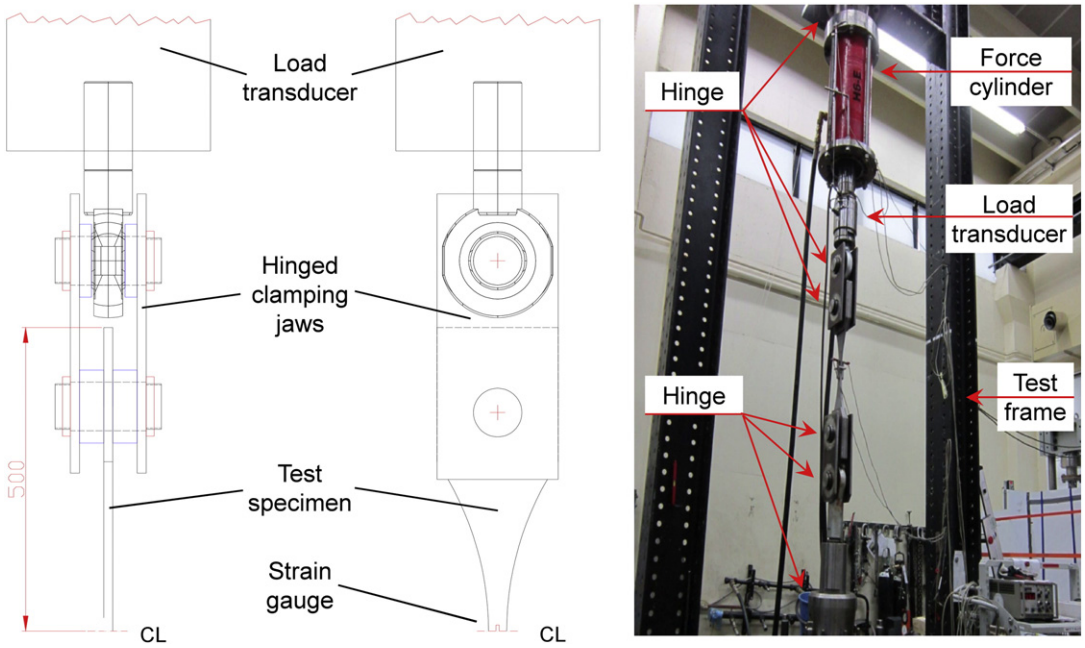

Fig. 7. Fatigue test setup.

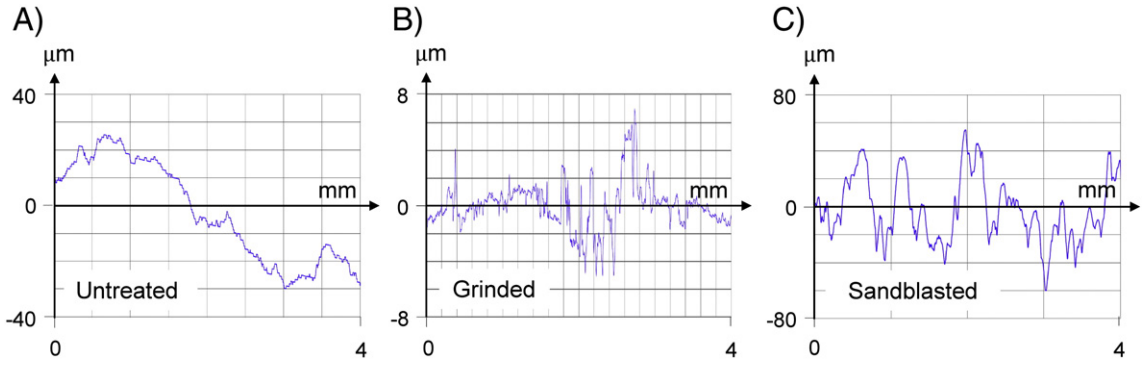

Fig. 8. Examples of surface profiles for plasma cut edge: A) untreated, B) grinded, and C) sandblasted.

specimens with a higher yield strength. In addition, the slope of the *S–N* curve increases with an increase in the yield strength. All the test results are well above the reference design curve of DNV [3]; corrosion protection is to be used, $N < 10^7$, $m = 4$, FAT160. For the specimens with a yield strength of 690 MPa, the fatigue strength is close to the measured monotonic yield strength of 744 MPa–843 MPa given in Table 2. The numerical values for the applied stress range and fatigue life are given in Appendix B.

In Fig. 14, the influence of different treatments on the fatigue strength and slope value has been compared for the series with a yield strength of 690 MPa. There a 97.7% probability of survival is considered. In this case, all the results are again well above the reference design curve [3]. When the specimens have been grinded or sandblasted after the grinding, the slope increases considerably when compared to the untreated specimens. All the fatigue strength curves meet at the range of 10^4 to 10^5 cycles, so that the *S–N* curve for the untreated specimens agrees with the slope of the design curve, $m = 4$. It can also be seen that grinding the specimens increases the fatigue strength, but sandblasting after grinding reduces the fatigue strength only slightly.

4.5. Fracture surfaces

On the basis of the fracture surface analysis, three different fatigue crack initiation types were observed: rolled plate surface, plate corner, and plasma-cut edge. Fig. 15 presents an example of each location of the fatigue crack initiation, while Table 3 summarises the crack initiation locations for all the test specimens. The untreated specimens showed a tendency for crack initiation from the rolled plate surface. In this case, several crack initiation locations were observed, as indicated by the ratchet marks in Fig. 16A. Grinding and sandblasting changed the behaviour

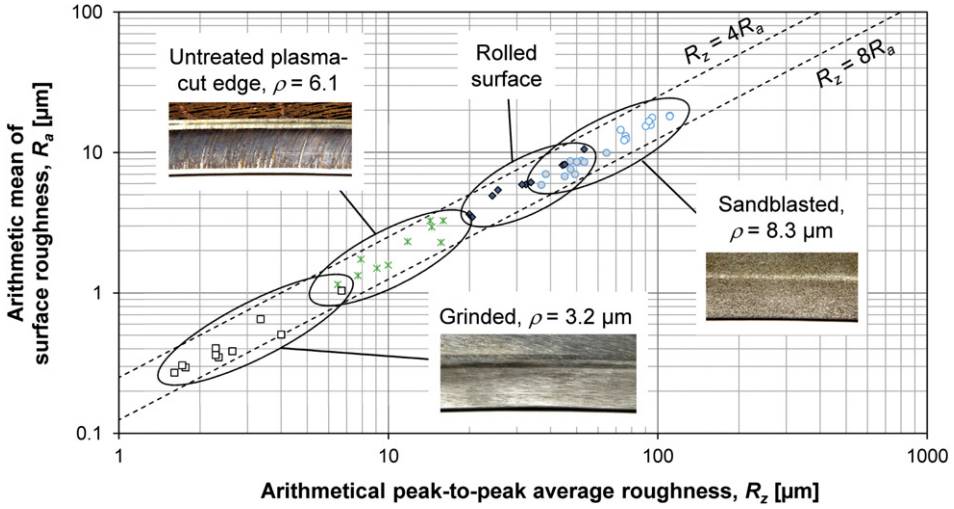

Fig. 9. Surface roughness and defect radius, ρ, for different surface treatments.

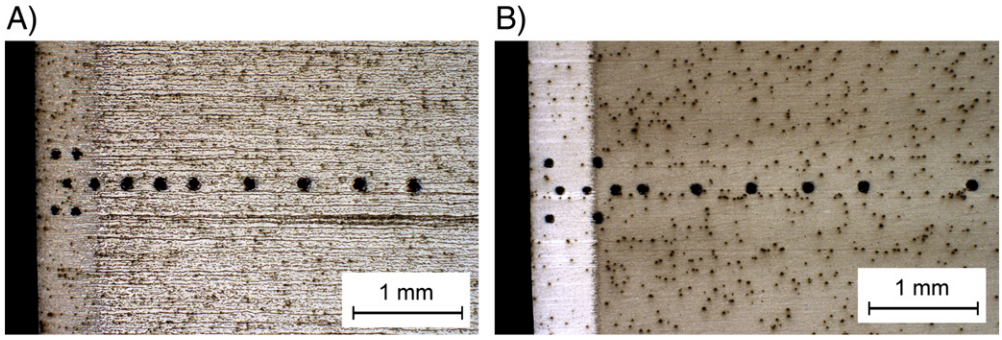

Fig. 10. Macro section of the untreated specimens with yield strengths of 460 MPa (A) and 690 MPa (B).

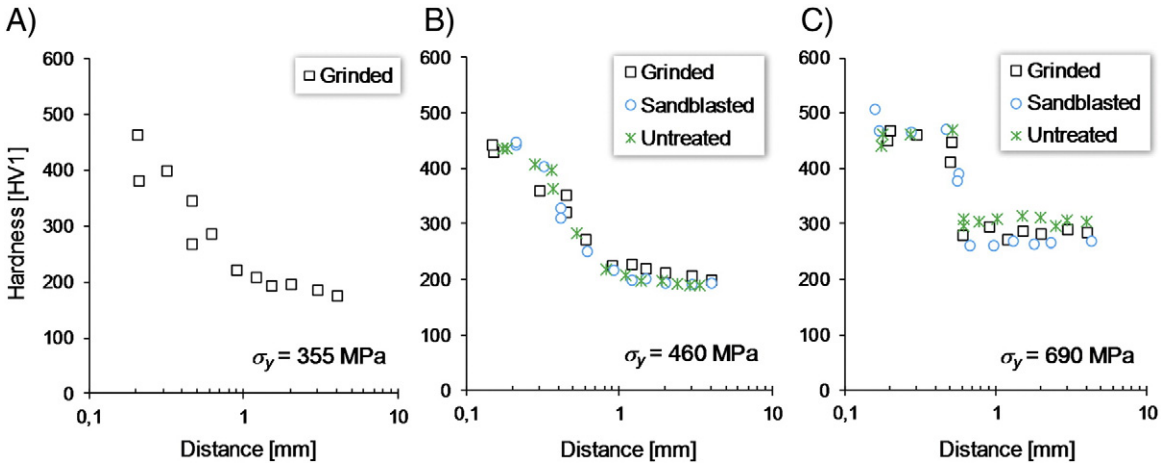

Fig. 11. Hardness for the specimens with a yield strength of 355 MPa (A), 460 MPa (B) and 690 MPa (C).

towards initiation in the corner of the plate. In the case of the sandblasted and grinded specimens with a yield strength of 460 MPa or 690 MPa, the cracks mainly initiated close to the interface of the base material and the heat-affected zone, which is seen as a lighter shade of grey at the cut edge in Fig. 16B. For grinded specimens with a yield strength of 355 MPa, the cracks had a tendency to initiate at the plasma-cut edge. Consequently, it can be concluded that surface treatment removed the defects from the rolled surface and the crack initiation location changed from the rolled surface to the plate corner or plasma-cut edge.

5. Discussion

The investigation shows that the fatigue strength of a large-scale structure can be greatly increased by surface treatment. The treatment removed the surface defects, resulting in higher fatigue strength and also differences in the location of the fatigue crack initiation. The best results in terms of fatigue strength are obtained by grinding the plasma-cut and rolled plate surface. The positive effects are slightly reduced by sandblasting, which is required before the steel plates are

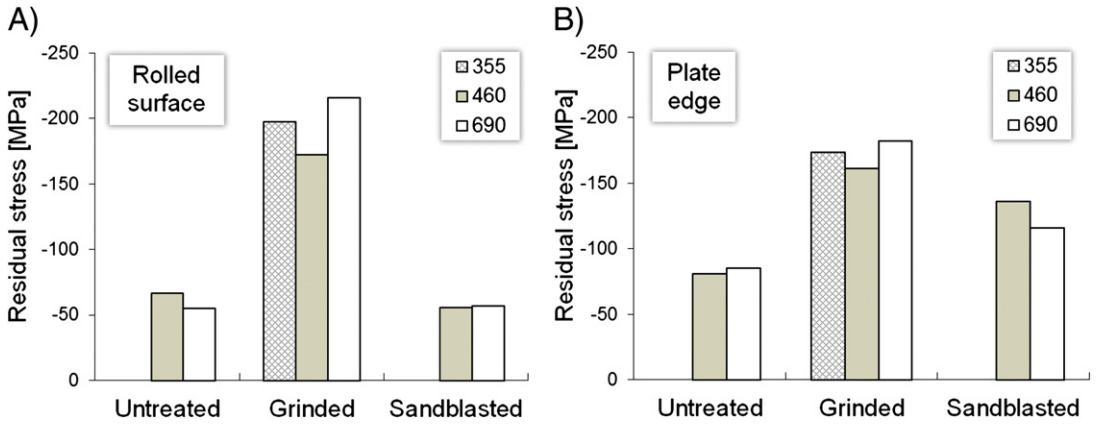

Fig. 12. Influence of the surface treatment on the maximum principal residual stress for the rolled plate surface (A) and plasma-cut plate edge (B).

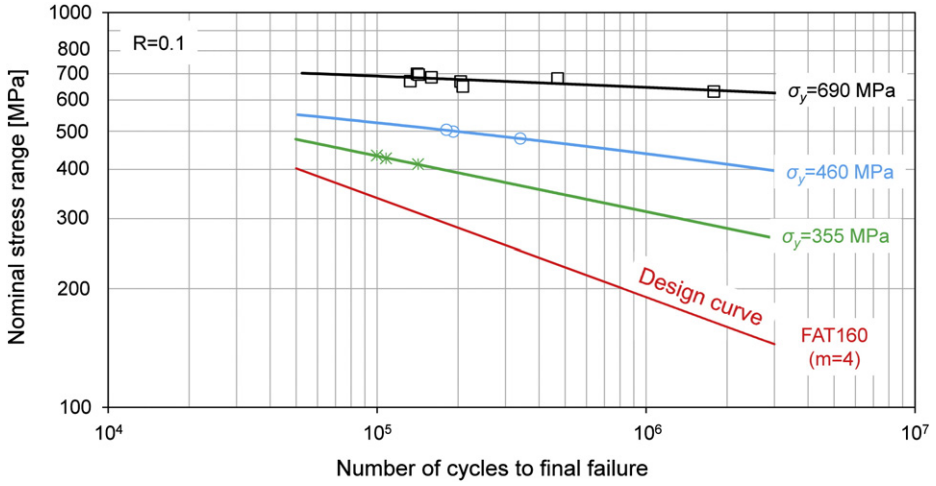

Fig. 13. Influence of material yield strength on the fatigue strength of the grinded specimens. The reference design curve [3] is given for comparison.

Table 2
Hardness-based estimation for the yield strength values of base material and their comparison with the measured values given in the steel producers' certificates.

Surface treatment	Nominal σ_y [MPa]	Hardness HV1	Estimated σ_y [MPa]	Measured σ_y [MPa]
Untreated	460	199	498	
Grinded	460	210	526	508
Sandblasted	460	205	513	
Untreated	690	299	747	
Grinded	690	300	750	744–843
Sandblasted	690	272	680	

Table 3
Crack initiation locations of the test specimens.

Surface treatment	Nominal σ_y	Fatigue crack initiation location		
		Rolled surface	Plate corner	Plasma-cut edge
Grinded	355	–	1	2
Untreated	460	3	–	–
Grinded	460	1	2	–
Sandblasted	460	–	3	–
Untreated	690	7	–	1
Grinded	690	2	6	–
Sandblasted	690	1	5	–

painted, because of the increased surface roughness and reduced compressive residual stress in comparison to the initial state after grinding; see Figs. 8, 9, and 12. However, sandblasting has a positive effect on the shape of the defects, making the notch radius larger. In addition, the surface treatment removed the defects from the rolled surface. As a result of these factors, the sandblasted specimens have a higher fatigue strength than the untreated specimens. These findings are supported by the investigations of Sasahara [6] and Ngiam and Brennan [15], who concluded that the better shape of the crack-like flaws and compressive residual stresses increases the fatigue strength.

The utilisation of the results depends on the statistical treatment of the experimental results. According to the design guidelines [3], the recommended slope value is $m = 4.0$ for the base material in a non-corrosive environment when the number of cycles is less than 10^7. The present results for the untreated specimens are in agreement with this, considering a safety factor of $f_s = 1.65$ between the design curve and tested specimens (97.7% probability level). However, for the grinded and sandblasted specimens the slopes observed in the tests are considerably higher than the slope $m = 4.0$. This is in line with the results of Gao et al. [7], who showed that with different surface treatments the slope is changed considerably in ultra-high-strength steel. Meanwhile, the results of this paper for the grinded specimens indicate that the slope value is also affected by the yield strength of the material when the specimens have a high surface quality. In this case, fitting the results to a fixed slope $m = 4$ leads to a situation where the scatter of the test results from the average curve becomes very high and the fatigue strength within the range of 10^4 to 10^5 cycles becomes higher than the measured yield strength of the material.

6. Conclusions

This paper investigated experimentally the influence of surface integrity on the fatigue strength of high-strength steel plates used in the balcony openings of cruise ship structures. Different surface treatments were considered to simulate the manufacturing process of the shipyard. The large-scale test specimens, which had a yield strength of 460 MPa or 690 MPa, were cut by plasma. After the cutting, the specimens were treated by grinding or by grinding followed by sandblasting. The resulting surface roughness, hardness, and residual stress were measured. Fatigue tests with a load ratio R = 0.1 were carried out.

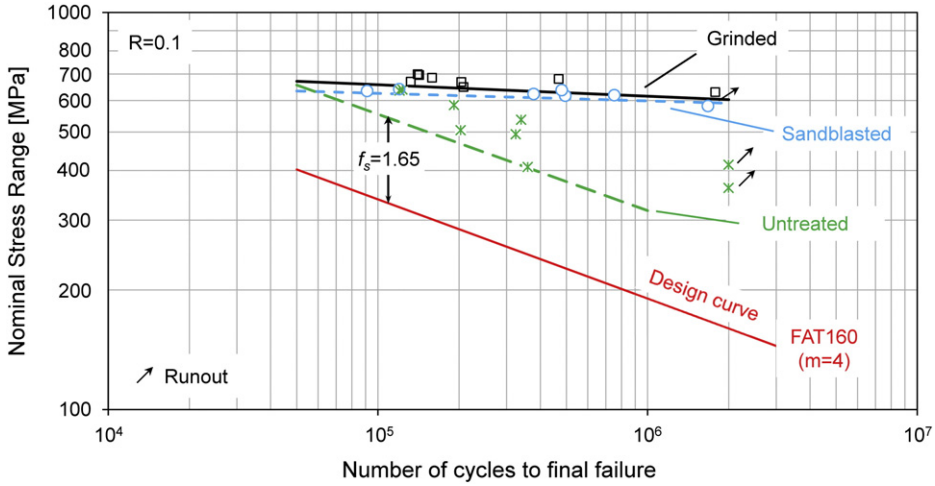

Fig. 14. Influence of surface treatment on fatigue strength of the specimen with yield strength of 690 MPa. The trend lines at a 97.7% probability of survival and reference design curve [3] are also given.

Fig. 15. Observed fatigue crack initiation locations: A) rolled surface, B) plate corner, and C) plasma-cut edge.

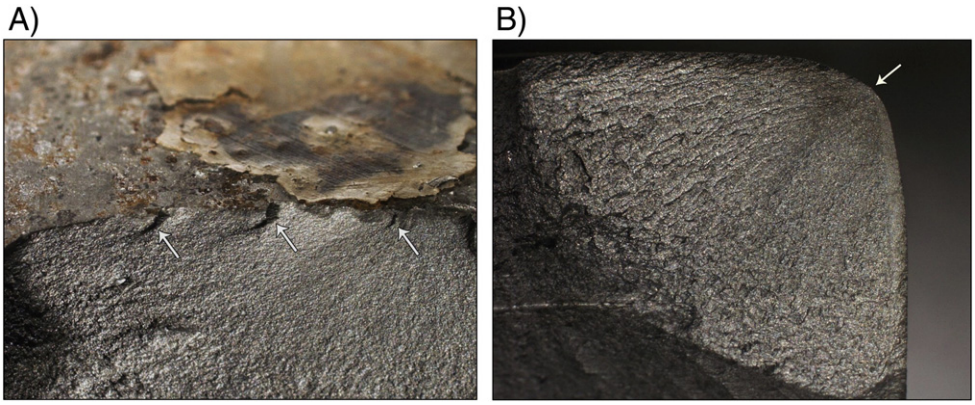

Fig. 16. Main difference in the fatigue crack initiation between untreated and treated specimens with yield strengths of 460 and 690 MPa: A) untreated plate surface with several crack initiation locations as indicated by the ratchet marks, and B) treated surface with one crack initiation location at the interface of the base material and heat-affected zone.

The investigation shows that post-cutting treatments suitable for shipyard conditions can considerably increase the fatigue strength of high-strength steel used in large-scale structures. The increase in fatigue strength is due to the reduced surface roughness and compressive residual stress. Sandblasting after grinding increases the surface roughness and reduces the compressive residual stress. However, the influence on the fatigue strength is minor since sandblasting produces a favourable defect shape that has a larger notch radius when compared to grinding. The surface treatment also has an influence on the slope of the *S–N* curve, which differs significantly from the commonly applied slope value $m = 4$.

The present study focused on the experimental investigation of the surface integrity and its influence on the fatigue strength of large-scale structures. Further analysis of the test results considering the theoretical modelling aspects is left for future work. In addition, the effect of the load history, i.e. variable amplitude loading, needs to be considered.

Acknowledgements

The research presented here was carried out in a Finnish research project funded by the Technology Agency of Finland, Tekes. The work is related to the Light and Innovations and Network projects within the scope of the Finnish Metals and Engineering Competence Centre. All the financial support is gratefully appreciated. Appreciation is also due to Akseli Kukkonen from the Department of Engineering Design and Production at Aalto University for his assistance.

Appendix A. Residual stress measurement data

The residual stress measurement data for the rolled surface and plasma-cut edge of the specimens with and without surface treatment are presented in Tables A-1 and A-2. In the residual stress measurement the interference line from {211} ferrite lattice plane ($2\theta = 156.4°$) was registered under 19 different χ-inclination angles: 0.0°, ±12.4°, ±17.6°, ±21.8°, ±25.4°, ±28.6°, ±31.7°, ±34.5°, ±37.3°, and ±40.0°. The exposure time for a single inclination was 5 s, and prior to the measurements a calibration measurement was made from a stress-free Fe powder. By applying Bragg's law, the bi-axial residual stresses were determined for the specimen surface. The calculated standard deviation of a single residual stress measurement was about 5 MPa.

Appendix B. Fatigue test results

Table B-1 summarises the specimen dimensions, applied load levels, stress range, and fatigue life for the final failure. If the fatigue life was longer than 2 million load cycles, the test was stopped and it was classified as a Run out test.

Table A-1
Residual stress measurement results, standard deviations, and principal stresses for the rolled surface of the specimens.

Surface treatment	Nominal σ_y	Residual stress [MPa]			Principal stress [MPa]		
		0° (x-direction)	45°	90° (y-direction)	σ_1	σ_2	φ
Grinded	355	−103.4 ± 5.3	−130.6 ± 3.5	−193.8 ± 2.6	−99.9	−197.2	−10°
Untreated	460	−66.1 ± 4.3	−45.1 ± 3.7	−32.6 ± 7.7	−32.1	−66.7	7°
Grinded	460	−49.3 ± 5.3	−91.2 ± 5.0	−169.8 ± 3.2	−46.6	−172.5	−8°
Sandblasted	460	−51.9 ± 2.5	−55.4 ± 2.9	−51.3 ± 2.3	−47.8	−55.5	−42°
Untreated	690	−54.9 ± 2.7	−44.9 ± 3.4	−34.7 ± 3.7	−34.7	−54.9	0°
Grinded	690	−110 ± 4.8	−148.7 ± 3.3	−214 ± 3.7	−108.3	−215.7	−7°
Sandblasted	690	−51.3 ± 2.5	−54.6 ± 2.5	−57.1 ± 2.6	−51.3	−57.1	3°

Table A-2
Residual stress measurement results, standard deviations, and principal stresses for the plasma-cut edge of the specimens.

Surface treatment	Nominal σ_y	Residual stress [MPa]			Principal stress [MPa]		
		0° (x-direction)	45°	90° (z-direction)	σ_1	σ_2	φ
Grinded	355	−81.6 ± 3.7	−127.7 ± 4.0	−174.1 ± 3.6	−81.6	−174.1	0°
Untreated	460	−8.3 ± 3.0	−45.2 ± 2.8	−81.1 ± 3.7	−8.3	−81.1	0°
Grinded	460	−76.8 ± 7.6	−125.2 ± 4.5	−160.6 ± 4.9	−76.2	−161.1	−4°
Sandblasted	460	−131.7 ± 2.4	−111.5 ± 3.0	−111.9 ± 3.9	−107.6	−136.1	23°
Untreated	690	−33.6 ± 3.0	−47.7 ± 2.6	−82.9 ± 5.4	−31.5	−85.1	−11°
Grinded	690	−63.8 ± 5.6	−127.7 ± 3.9	−182.3 ± 2.0	−63.6	−182.4	2°
Sandblasted	690	−115.7 ± 2.5	−103.6 ± 2.4	−92.9 ± 2.2	−92.8	−115.8	−1°

Table B-1
Summary of fatigue test results.

Yield strength	Surface treatment	Specimen name	Plate thickness	Width, w	Load ratio	Max. load	Min. load	Mean load	Stress range	Fatigue life
355	Grinded	P2_355_1	17.2	30.4	0.10	203	21	112	349	Run out
		P2_355_2	17.1	30.2	0.10	245	25	135	427	107,852
		P2_355_3	17.1	30.1	0.10	248	25	136	434	99,839
		P2_355_4	17.5	30.2	0.10	241	24	132	412	141,924
460	Untreated	P1_460_1	15.3	30.4	0.10	200	21	111	386	Run out
		P1_460_2	15.2	30.5	0.10	210	22	116	409	Run out
		P1_460_3	15.1	30.4	0.10	230	24	127	450	128,052
		P1_460_4	15.3	30.1	0.10	221	22	121	432	345,089
		P1_460_5	15.1	30.5	0.10	221	22	122	431	406,532
	Grinded	P2_460_1	15.0	30.1	0.10	240	24	132	479	340,454
		P2_460_2	14.9	30.3	0.10	250	25	137	499	191,725
		P2_460_3	14.8	30.1	0.10	249	25	137	504	180,729
	Grinded and sand-blasted	P3_460_1	15.1	30.2	0.10	230	23	126	455	132,519
		P3_460_3	15.0	30.0	0.10	220	22	121	440	Run out
		P3_460_4	15.1	30.3	0.10	225	22	124	444	133,496
		P3_460_5	15.0	30.4	0.10	225	22	124	445	1,683,779
690	Untreated	P1_690_1	15.1	30.4	0,08	255	21	138	511	200,710
		P1_690_2	15.3	30.5	0,09	210	19	115	409	359,047
		P1_690_3	15.1	30.4	0.10	183	18	101	360	Run out
		P1_690_4	15.4	30.5	0.10	259	26	142	497	322,686
		P1_690_5	15.1	30.4	0.10	210	21	116	411	Run out
		P1_690_6	15.3	30.6	0.10	281	28	154	540	338,862
		P1_690_7	15.1	30.1	0.10	240	25	133	475	555,330
		P1_690_8	15.4	30.6	0.10	340	33	187	650	118,407
		P1_690_9	15.2	31.0	0,11	310	35	173	584	190,356
		P1_690_10	15.1	31.0	0.10	340	35	188	654	122,227
	Grinded	P2_690_1	14.9	30.2	0.10	335	34	184	670	132,574
		P2_690_2	15.0	30.5	0.10	340	34	187	669	204,120
		P2_690_3	14.9	30.7	0.10	320	32	176	630	1,784,428
		P2_690_4	15.0	30.1	0.10	350	35	192	700	140,676
		P2_690_5	15.0	30.6	0.10	349	35	192	685	159,009
		P2_690_6	14.9	30.1	0.10	340	34	187	680	468,579
		P2_690_7	15.0	30.4	0.10	330	34	182	649	207,989
		P2_690_9	15.1	30.1	0.10	350	35	193	696	142,475
	Grinded and sand-blasted	P3_690_4	15.0	30.0	0.10	290	29	160	580	Run out
		P3_690_5	15.1	30.5	0.10	330	33	182	647	119,358
		P3_690_6	14.9	30.2	0.10	320	32	176	638	90,681
		P3_690_7	15.0	30.4	0.10	310	31	171	613	752,909
		P3_690_8	15.1	30.3	0.10	315	31	173	624	377,856
		P3_690_9	15.1	30.5	0.10	315	32	173	618	495,229
		P3_690_10	15.0	30.1	0.10	320	32	176	639	479,482

References

[1] Sharp JV, Billingham J, Stacey A. Performance of high strength steels used in jack-ups. Mar Struct 1999;12(4):349–70.
[2] Miki C, Homma K, Tominaga T. High strength and high performance steels and their use in bridge structures. J Constr Steel Res 2002;58(1):3–20.
[3] Det Norske Veritas. Classification notes. Fatigue Assessment of Ship Structures, No. 30.7. Hovik, Norway: Det Norske Veritas; 2008 .
[4] Sperle J-O. Influence of parent metal strength on the fatigue strength of parent material with machined and thermally cut edges. Weld World 2008;52(7–8): 79–92.
[5] Murakami Y, Endo M. Effect of defects, inclusions and inhomogenities on fatigue strength. Int J Fatigue 1994;16(3):163–82.
[6] Sasahara H. The effect on fatigue life of residual stress and surface hardness resulting from different cutting conditions of 0.45%C steel. Int J Mach Tools Manuf 2005;25:131–6.
[7] Gao Y, Li X, Yang Q, Yao M. Influence of surface integrity on fatigue strength of 40CrNi2Si2MoVA steel. Mater Lett 2007;61:466–9.
[8] Ryu HR, Kim WS, Ha HI, Kang SW, Kim MH. Effect of toe grinding on fatigue strength of ship structure. J Ship Prod 2008;24(3):152–60.
[9] Jesus AMP, Matos R, Fontoura BFC, Rebelo C, Silva LS, Veljkovic M. A comparison of the fatigue behavior between S355 and S690 steel grades. J Constr Steel Res 2012;79:140–50.
[10] Bäcktröm M, Kivimaa S. Estimation of crack propagation in a passenger ship's door corner. Ships Offshore Struct 2009;4(3):241–51.
[11] SFS-EN ISO 4288. Geometrical Product Specifications (GPS) — surface texture: profile method — rules and procedures for the assessment of surface texture; 1996 .
[12] SFS-EN ISO-6507. Metallic materials. Vickers hardness test. Part 1: test method; 2005 .
[13] Pavlina EJ, Van Tyne CJ. Correlation of yield strength and tensile strength with hardness for steels. J Mater Eng Perform 2008;17(6):888–93.
[14] EN 15305:2008. Non-destructive testing—test method for residual stress analysis by X-ray diffraction. Brussels, Belgium: European Committee for Standardisation; 2008 .
[15] Ngiam SS, Brennan FP. Fatigue crack control in structural details using surface peening. J Ship Prod 2008;24(3):147–51.